Chemical Society Reviews TUTORIAL REVIEW

Recognition and Applications of Anion–Anion Dimers based on Anti-Electrostatic Hydrogen Bonds (AEHBs)

Received 00th January 20xx, Accepted 00th January 20xx

DOI: 10.1039/x0xx00000x

Wei Zhao, Amar H. Flood, a* and Nicholas G. Whiteb*

Based on Coulomb's Law alone, electrostatic repulsion between two anions is expected to prevent their dimerization. Contrary to that idea, this *Tutorial Review* will present evidence showing that anion-anion dimers of protic hydroxyanions can form readily, and describe conditions that facilitate their formation. From X-ray crystal structures, we learn that hydroxyanions dimerize and oligomerize by overcoming long-range electrostatic opposition. Common examples are hydroxyanions of phosphate, sulfate, and carbonate, often in partnership with charged and neutral receptors. Short-range hydrogen bonds between anionic donors and acceptors are defined as *anti*-electrostatic hydrogen bonds (AEHBs) with insight from theoretical studies. While anion dimers are difficult to identify unequivocally in solution, these solution dimers have recently been definitively identified. The development of the supramolecular chemistry of anion-anion dimers has led to applications in hierarchical assemblies, such as supramolecular polymers and hydrogen bonded organic frameworks.

Learning points

- 1. *Anti*-electrostatic hydrogen bonds (AEHBs) occur within anion-anion dimers (and oligomers and polymers) composed of protic hydroxyanions where attractive contacts offset Coulombic repulsions at short range.
- 2. Anion-anion dimers can be stabilized in solids and solutions by proximal cations and by complementary anion receptors.
- 3. Signatures of anion-anion dimers are short O–H···O contacts in crystal structures with O···O distances of 2.5–2.7 Å, and down-field 12–16 ppm resonances in solution NMR spectra.
- 4. Anion-anion dimers connected by AEHBs have a growing set of applications in crystal engineering, supramolecular polymers, and CO_2 capture.
- 5. AEHBs are emerging as a predictable design motif for use in the design and construction of hierarchical supramolecular assemblies.

1. Introduction

The recognition of anions by synthetic receptors has been a major focus of supramolecular chemistry over the past few decades and has resulted in significant advances and applications in a range of fields.¹ Chemists have concentrated on using neutral or cationic receptors to bind a single anion in an effort to maximise favourable electrostatic attractions. When binding more than one anion, receptors have typically incorporated well-separated binding pockets to minimise unfavourable anion…anion repulsions. This common-sense strategy has clear merits. Nature, however, offers clues that under certain circumstances anion…anion contacts may not always be so unfavourable. For example, phosphate binding proteins contain an anionic carboxylate residue, which is

In recent years, there has been a surge of interest in the use of *anti*-electrostatic hydrogen bonds† (AEHBs) in supramolecular chemistry, i.e., deliberately forming hydrogen bonds between anions. This usage often leads to the formation of dimers (Fig. 1a-c), although in cases where the anion has more than one hydrogen atom, such as H₂PO₄⁻, it also becomes possible to form trimers, clusters and polymeric structures (Fig. 1d).

Fig. 1 Common anion–anion AEHB interactions: a) HCO_3^- dimer; b) HSO_4^- dimer; c) $H_2PO_4^-$ dimer; d) $H_2PO_4^-$ 1D polymer.

This Tutorial Review will provide an overview of AEHBs and the anion-anion dimers they stabilize, their characterization from initial crystallographic, physical organic and computational studies through to the current state-of-the-art in molecular recognition. It is thought that short range attractions from hydrogen bonding inside anion-anion dimers and the attractions between the anion dimers and receptors, offset the long-range repulsions between anions in the dimers. Although common wisdom leads us to think of these types of AEHBs as "weak," it is surprising to find that these interactions are strong enough to drive hierarchical assemblies in both the solid-state and in solution. We will highlight opportunities when using this new recognition motif to form supramolecular polymers, in anion transport and even in CO₂ capture. By taking advantage of these reliable interactions, and the ability to manipulate them at the molecular level, we expect to see more applications of AEHBs emerge soon.

believed to give these proteins their selectivity for phosphate over sulfate.² This selectivity emerges because, at biological pH, phosphate's hydroxyl group(s) (–OH) can form a hydrogen bond to the carboxylate residue.

^{a.} Department of Chemistry, Indiana University, 800 East Kirkwood Avenue, Bloomington, IN 47405, USA. Email: aflood@indiana.edu. Web: www.floodweb.sitehost.iu.edu

b. Research School of Chemistry, Australian National University, Canberra, ACT, Australia. Email: nicholas.white@anu.edu.au. Web: www.nwhitegroup.com.

2. AEHB anion---anion dimers in the solid state

Solid state X-ray crystal structures of anion---anion dimers, and higher-order aggregates such as trimers, tetramers and polymers have been known for a long time. One of the earliest structures from 1961 shows short hydrogen bonds between the negatively-charged ends of the aminoethylphosphate zwitterion (Fig. 2a). Formation of the AEHBs between the negatively charged ends should confront every assumption held about Coulombic repulsion and attraction. Based solely on electrostatics, the negative phosphate should be associated with the positively charged ammonium. Another early crystal structure of an AEHB anion---anion network was reported in 1972 by Hearn and Bugg. This structure of ephedrine dihydrogen phosphate features a two dimensional (2D) sheet of H_2PO_4 - anions assembled through AEHBs (Fig. 2b).

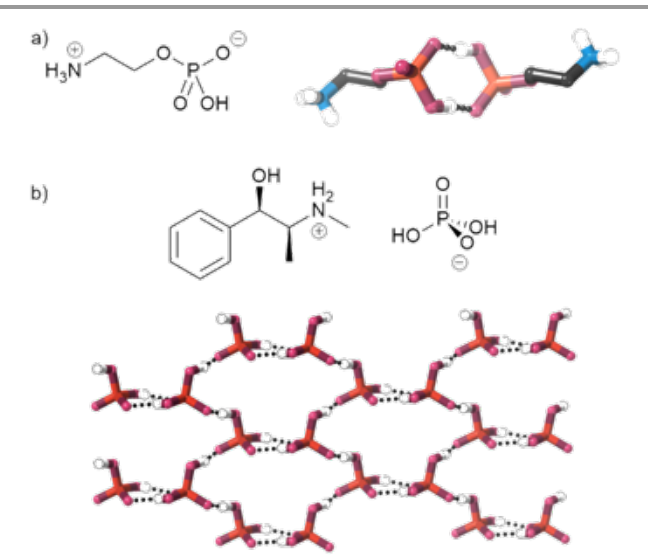


Fig. 2 Early examples of solid-state AEHB interactions characterised by X-ray crystallography: a) Kraut's structure of the 2-aminoethylphosphate zwitterion, 3 which has short hydrogen bonding between the negatively-charged parts of the molecule (CSD: AEPHOS); b) AEHB contacts in a $\rm H_2PO_a^{-}2D$ sheet from the structure of ephedrine dihydrogen phosphate (CSD: EPHDHP).⁴

These interactions are relatively commonly in solids. In 2013, Rajbanshi, Custelcean and co-workers reported an analysis of the Cambridge Structural Database (CSD) looking at interactions between $H_2PO_4^-$ anions.⁵ They considered any case where a $H_2PO_4^-$ anion formed a hydrogen bond with another $H_2PO_4^-$ and found almost all phosphates form dimers or larger aggregates with only about 5% truly monomeric. Approximately 12% of structures contained the archetypal $H_2PO_4^-$ dimer (Fig. 3), where each anion gives and receives a hydrogen bond, while in a further 31% of structures a 1D chain was observed where each anion gives and receives a hydrogen bond (Fig. 3).

In 2016, Fatila, Flood and colleagues noted that there were more than 80 examples of HSO₄⁻ dimers in the CSD,⁶ and a 2018 review by He, Tu and Sessler⁷ highlighted many crystal structures of AEHB dimers, trimers, tetramers and clusters. In 2019, White surveyed the CSD for AEHB interactions between a range of protic anions to investigate just how commonly these interactions occurred. Despite the relatively strict criterion that each anion must both give and receive a hydrogen bond, a large number of structures containing such interactions were found.⁸

Notably, more than a third of crystal structures containing $H_2PO_4^-$ anions, and more than half containing bicarbonate anions (HCO₃⁻) exist in this form. In addition, dimers of $H_2AsO_4^-$ and $HSeO_4^-$ were observed, as well as "highly *anti*-electrostatic" dimers between dianions of phosphate [HPO₄²⁻···HPO₄²⁻] and of arsenate [HASO₄²⁻···HASO₄²⁻].

Fig. 3 Representation of the most common H-bonding arrangements observed by Custelcean, the percentage given is the proportion of structures in the CSD (in 2013) with this interaction. For reference, only about 5% of $H_3PO_4^-$ anions were found to be discrete (*i.e.*, monomeric) anions. A double line indicates that the anion both gives and receives a hydrogen bond, while a single line indicates a single hydrogen bond; a dashed line indicates a polymeric structure.

The oxygen—oxygen distances in the dimers were surprisingly consistent, clustered around 2.60 Å. This distance is similar to, or slightly shorter than the oxygen—oxygen distances observed in carboxylic acid dimers, which do not have to contend with Coulombic repulsion. Small, but statistically significant, differences were observed between the mean interaction length in dimers of $H_2PO_4^-$, HCO_3^- and HSO_4^- at 2.585(2), 2.606(2) and 2.620(3) Å, respectively (Fig. 4). White attributed the shorter distance in $H_2PO_4^-$ dimers to this anion being in a "Goldilocks" region where the H-atoms are relatively acidic, while the O-atoms are appreciably basic.8 Interestingly, there was no difference in the oxygen—oxygen interaction distances between complexes of anions coordinated to metal cations compared with non-coordinated anions.

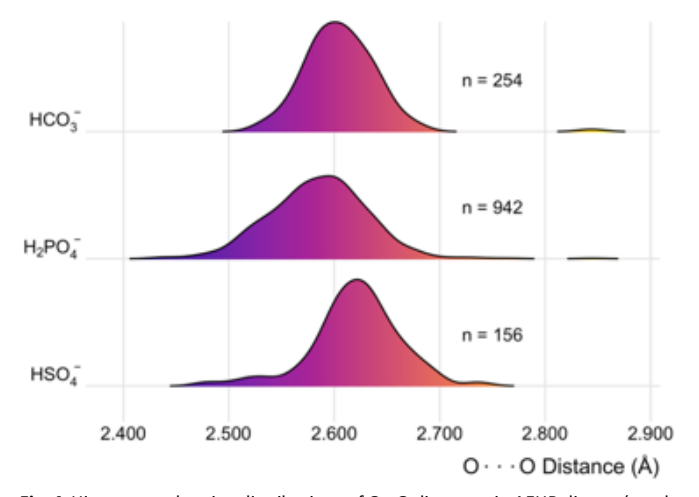


Fig. 4 Histograms showing distributions of $0\cdots 0$ distances in AEHB dimers (n = the number of interactions in the CSD for each anion). Adapted from Ref. 8 with permission from the Royal Society of Chemistry.

Journal Name ARTICLE

The CSD was also searched for heterodimers. Only one was found: a trimer consisting of two HSO_4^- anions sandwiching a central $H_2PO_4^-$ anion reported by Light and Gale (Fig. 5).⁹ The O···O distances in this trimer are very short (indeed two of the shortest in White's CSD survey), and this may stem from a combination of the relatively acidic hydrogen atom present in HSO_4^- anions ($pKa_2 = 1.9$) and the basic oxygen atoms in the central dihydrogen phosphate ($pKa_2 = 7.2$).

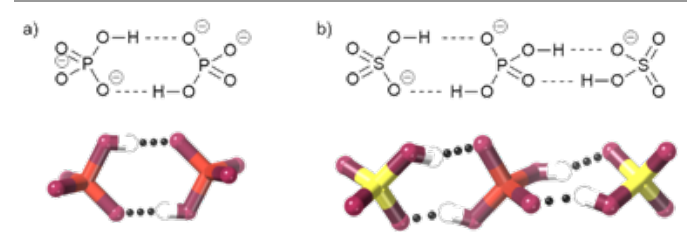


Fig. 5 Examples of unconventional AEHB complexes in the CSD: a) a highly *anti*-electrostatic dimer of dianions to make a tetraanionic [HPO4:-HPO4] 4 - dimer (CSD: FUJPEF) and b) Light and Gale's heterotrimer (CSD: IQOKOQ). 9

3. Theoretical studies of anion---anion dimers

The first computational studies of hydrogen bonded complexes between anions were conducted by Braga, Grepioni and Novoa in 1998.10 They studied the bioxalate anion (Fig. 6) in the gas phase and compared this to the crystal structure of potassium bioxalate. Their calculations showed the interaction between bioxalate anions to be repulsive. For this reason, they concluded that the hydrogen bonds observed in X-ray crystal structures of such systems should be regarded as "pseudo-hydrogen bonds" capable only of organizing structures. They suggested that this interaction acts as a "tugboat" that does not link the ions, but rather minimizes the penalty of the close anion...anion contacts resulting from highly favourable potassium...anion interactions. However, Steiner,¹¹ and Mascal and co-workers¹² questioned these findings on crystallographic grounds, 11,12 and on the basis of ¹H NMR experiments showing evidence for bioxalate selfassociation in chloroform.¹² It was suggested that the model provided by Novoa was "not an ideal representation, since it does not predict the observed association."12

In 2005, Kass conducted gas phase DFT studies on a range of anionic and zwitterionic species and noted that while it was favourable for pairs of anions to dissociate, in several cases there was a significant barrier to dissociation. This barrier could be as high as 40 kJ mol⁻¹ for the complex between the mono-anion of naphthalenedicarboxylic acid and chloride. While larger aggregates (trimers and tetramers) were highly unstable, local minima were readily found. Kass highlighted that, given the charged nature of amino acids and proteins, these interactions may be important in biological processes.

After something of a lull in this area of research, DFT calculations of the $H_2PO_4^-$ dimer published by Mata, Espinosa and colleagues in 2012 provided additional detail.¹⁴ These calculations revealed that, while the gas phase interaction between the two anions was fundamentally unfavourable,

there was a region of stability such that when the two anions were relatively close together, an AEHB dimer was metastable with a 61 kJ mol $^{-1}$ barrier to dissociation (Fig. 6). This outcome occurs when the two anions are very close such that the phosphorus atoms of the anions are separated by 3–7 Å. Taken together these studies indicate that $\rm H_2PO_4^-$ dimers (and larger assemblies) may well be stable in solution and the solid state. Espinosa attributed this stability to favourable hydrogen bonding involving a significant sharing of charge. $\rm ^{14}$

Weinhold and Klein subsequently showed a range of anions could form metastable gas-phase dimers. While they are less stable than at infinite separation, there is a significant local minimum in some of the potential-energy surfaces. 15 Thus, as observed by Kass¹³ and Espinosa,¹⁴ once the anions are brought close together, they remain stable. Weinhold showed some AEHB dimers possess only a shallow energy well, for example, the F^- ... HCO_3^- complex has a well-depth of < 1 kJ mol^{-1} . However, simply replacing HCO₃⁻ with the glycolate anion (i.e., replacing HO-CO₂- with HO-CH₂-CO₂-) substantially increased the well depth to 15 kJ mol-1. This outcome arises from a combination of the insulating effect of the CH₂ group protecting the H-bonding OH group from the negatively charged CO₂- part of the molecule, and the extra distance reducing the effect of the repulsive sites. The theoretical studies of the homo-dimers of bicarbonate, bioxalate and terephthalate (Fig. 6) revealed they had well depths of 9, 23 and 52 kJ mol⁻¹, respectively.¹⁵

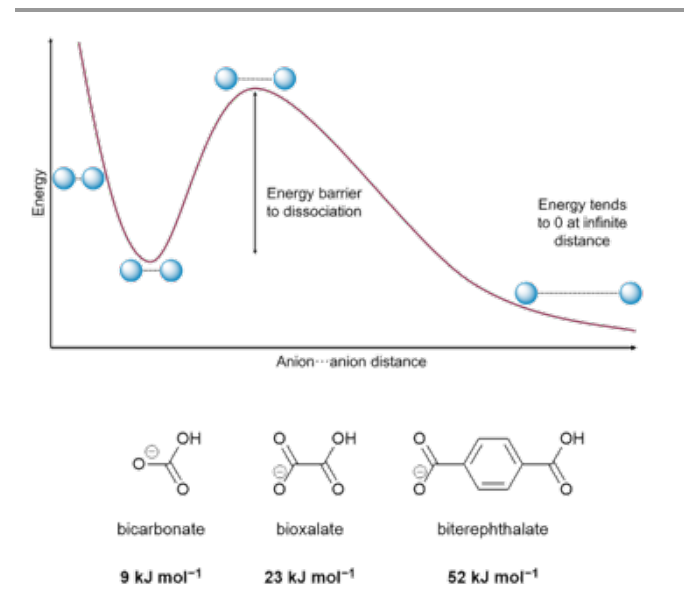


Fig. 6 Schematic indicating region of metastability seen in gas-phase calculations of AEHB dimers. Energy barriers to dissociation calculated by Weinhold for three carboxylate anions are provided. 15

Subsequent studies by Alkorta and colleagues compared the hydrogen bonding interaction between neutral dimers of carbonic acid and anti-electrostatic dimers of bicarbonate, e.g., between the $(H_2CO_3)_2$ and $(HCO_3^-)_2$ dimers, as well as between longer carboxylate and carboxylic acids containing additional methylene groups. ¹⁶ Based on detailed comparisons of the energetic properties, the authors concluded that the nature of

the H-bonding in AEHB dimers is the same as neutral dimers, it is only the Coulombic repulsion (or lack of it) that differs. Importantly, calculations using a polarizable continuum model to approximate aqueous solutions suggest that solvent can effectively screen the repulsive Coulombic interaction, increasing the stability of the AEHB dimer.¹⁷ A similar outcome is seen when simple cations (Na⁺, Mg²⁺) are present in these calculations. It is, therefore, not unreasonable to think that well-designed receptors may be able to screen the charge even more effectively and further stabilize AEHB dimers in solution.

4. Anti-Electrostatic Hydrogen Bonds and Anion– Anion Dimers in Solution

4.1 Early studies

In 1987, Cerrata and Berglund used Raman spectroscopy to characterize associations of dihydrogen phosphate in water. 20 By increasing concentration from 0.1 M to supersaturated 5 M aqueous solutions, the intensity of the symmetric stretch of P–(OH) $_{\rm 2}$ at 875 cm $^{-1}$ increases and the asymmetric stretch band of P=O at 1075 cm $^{-1}$ decreases. These changes were attributed to hydrogen bonded phosphate-phosphate associations at high concentrations.

In the early 1990s, the possibility that phosphate dimers may be important species when studying anion recognition began to be considered. Flatt, Lynch and Anslyn suggested that neutral phosphate esters may dimerize in the presence of a receptor containing a polyaza cleft.21 Valiyaveettil, Reinhoudt and coworkers used these findings to postulate that a series of tripodal amide receptors with the general structures 1 and 2 (Fig. 7) bound a H₂PO₄- dimer, based on an observed host:guest stoichiometry of 1:2 for the addition of H₂PO₄- but 1:1 for the addition of Cl⁻ and HSO₄⁻ in chloroform.²² Interestingly, changing the solvent to acetonitrile changed the H₂PO₄- binding stoichiometry to 1:1. While the hypothesis that the receptor was binding an anion-anion dimer in chloroform is certainly plausible, other explanations for the observed stoichiometry are also reasonable, such as more than one anion interacting with different parts of the polydentate hosts.

Fig. 7 General structure of Reinhoudt's tripodal receptors, which were suggested to bind $\rm H_2PO_4^-$ dimers. 22

Since these studies, a growing body of evidence has accumulated in favour of receptor-stabilized anion—anion dimers in solution. With the benefit of hindsight, it is likely that the hosts discussed in the subsequent section genuinely interact with anion—anion dimers. However, it is important to remember that until recently the presence of such interactions had not been definitively established. As a result, many of the authors were understandably cautious in their claims of anion—anion associations.

4.2 Crystal Structures of Receptor-stabilized Anion-Anion Dimers

Well-designed receptors offer a powerful way to stabilize anion dimers by offsetting electrostatic repulsion. Early examples of receptor-stabilized anion—anion associations are supported by crystal structures. These early reports have been recently reviewed by He and Sessler in 2018,⁷ and for this reason we only select four examples to reflect the signatures of receptor-stabilized anion—anion dimers. While these structures show receptor-stabilized anion—anion dimers in the solid state, in many cases it is not clear whether they persist in solution or they are instead induced by the crystallization process.

Many examples of neutral receptors supporting anionanion associations have been reported that rely upon strong hydrogen bond donors for anion binding. In 2010, Wang and Yan²³ reported dihydrogen phosphate dimers co-crystallized with four indolocarbazole-based neutral receptors **3** (Fig. 8a), in which two hydrogen bonds were seen between the receptor's NH groups and phosphate, and two AEHBs were seen between two phosphate anions. Urea is also widely used as a hydrogen-bond donor for anion receptors. A crescent urea chelator **4** (Fig. 8b) designed by Chutia and Das²⁴ in 2014 stabilized a bicarbonate dimer through hydrogen bonding and halogen bonding in a 4:2 receptor:bicarbonate stoichiometry. A sophisticated oligourea receptor **5** (Fig. 8c) studied by Wu and co-workers²⁵ showed encapsulation of a phosphate dimer in a 1:2 receptor:phosphate stoichiometry in the solid state.

Akin to ionic stabilization from countercations, positively charged receptors are an ideal way to stabilize anion-anion dimers in the solid state. A recent example from 2016, González Caballero, Alkorta, Molina and coworkers²⁶ reported a bistriazolium-based receptor **6** (Fig. 8d) interacting with anion dimers by charge-assisted hydrogen bonding. Their crystal structures show two dihydrogen pyrophosphate anions dimerized together with quadruple AEHBs co-stabilized by two cationic receptors. The authors obtained evidence that these interactions persist in solution, with both computational studies and diffusion ordered spectroscopy (DOSY) NMR studies suggesting the presence of two receptors assembled around a H₂P₂O₇²-·····H₂P₂O₇²- dimer. It is notable that the O···O AEHB

Journal Name ARTICLE

distances in these four systems (3–6) are all within the "normal" range identified in Fig. 4 (2.52–2.64 Å).

Along with the broad development of anion recognition, more sophisticated receptors have been found to stabilize anion-anion dimers in solution. In the following section, we will review key developments and efforts to characterize the AEHBs and anion associations in solution using UV-Vis spectroscopy, mass spectrometry, and isothermal calorimetry (ITC).

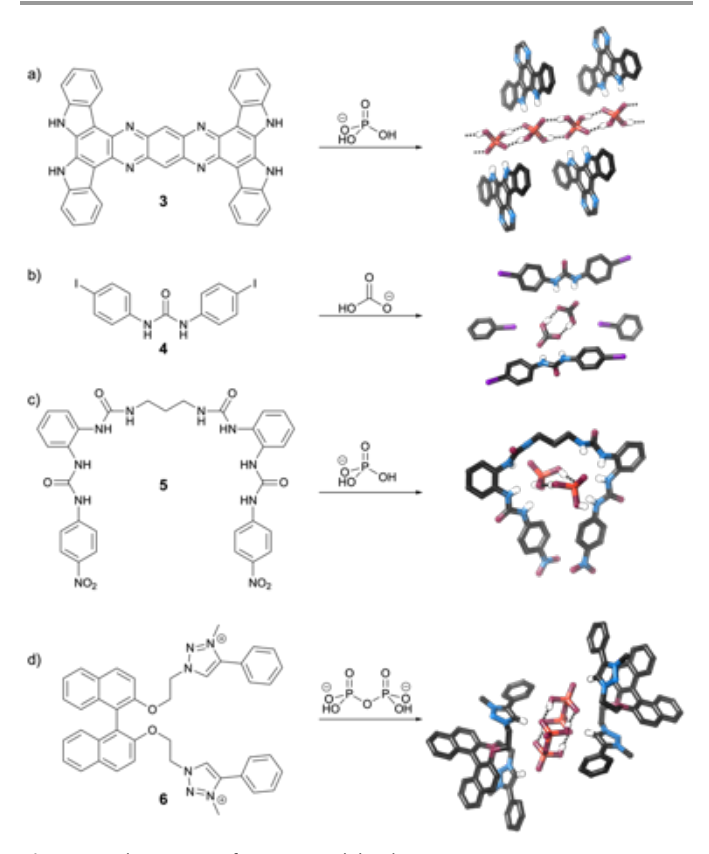


Fig. 8 Crystal structures of receptor-stabilized AEHB anion-anion association using a) neutral indolocarbazole receptors for a $H_2PO_4^-$ dimer (CSD: TUVDEU);²³ b) crescent urea receptor for the bicarbonate dimer (CSD: CONMOJ);²⁴ c) flexible oligourea receptor for a $H_2PO_4^-$ dimer (CSD: JUSMER);²⁵ d) cationic bis-triazolium chelator for dihydrogen pyrophosphate dimer (CSD: URUCOB).²⁶

4.3 UV-Vis Spectroscopy of Anion-Anion Dimers

In 2002, an early study by Kubo and coworkers²⁷ proposed receptor-stabilized phosphate dimers in acetonitrile. The Job plot indicates a 1:2 receptor-anion complex between the positively-charged isothiouronium receptor **7** (Fig. 9a) and phosphate anions. The authors proposed that the first $H_2PO_4^-$ anion binds to the receptor through charge-assisted hydrogen bonding, and a second $H_2PO_4^-$ anion interacts with the first $H_2PO_4^-$ anion through AEHBs. A similar mechanism was proposed by Baggi, Fabbrizzi and colleagues²⁸ using a ureabased cationic receptor **8** in acetonitrile (Fig. 9b). Multiple changes in the UV-Vis spectra seen during titration with the $H_2PO_4^-$ anion indicate multiple equilibria occur consistent with the proposed 1:2 binding event between receptor and $H_2PO_4^-$ dimers.

Recently, He, Sessler and coworkers²⁹ observed similar UV-Vis spectroscopic changes upon titration of monohydrogen pyrophosphate, HP₂O₇³⁻, into a solution of calix[4]pyrrole-based bismacrocycle receptor **9** in 1,2-dichloroethane (Fig. 9c). The 1:2 complex indicated by UV-Vis spectroscopy is consistent with the crystal structure of **9** and H₂P₂O₇²⁻ dimers, where proton transfer occurred in the crystallization process from HP₂O₇³⁻ to form the dihydrogen dianion, H₂P₂O₇²⁻. Quadruple AEHBs hold the H₂P₂O₇²⁻ dimer together under confinement by **9**. Interestingly, they also found that the bismacrocycle **9** can encapsulate H₂PO₄⁻ dimers and SO₄²⁻ dimer, although these anions are bridged by water molecules and thus do not have the archetypal anion—anion dimer structure shown in Fig. 1.

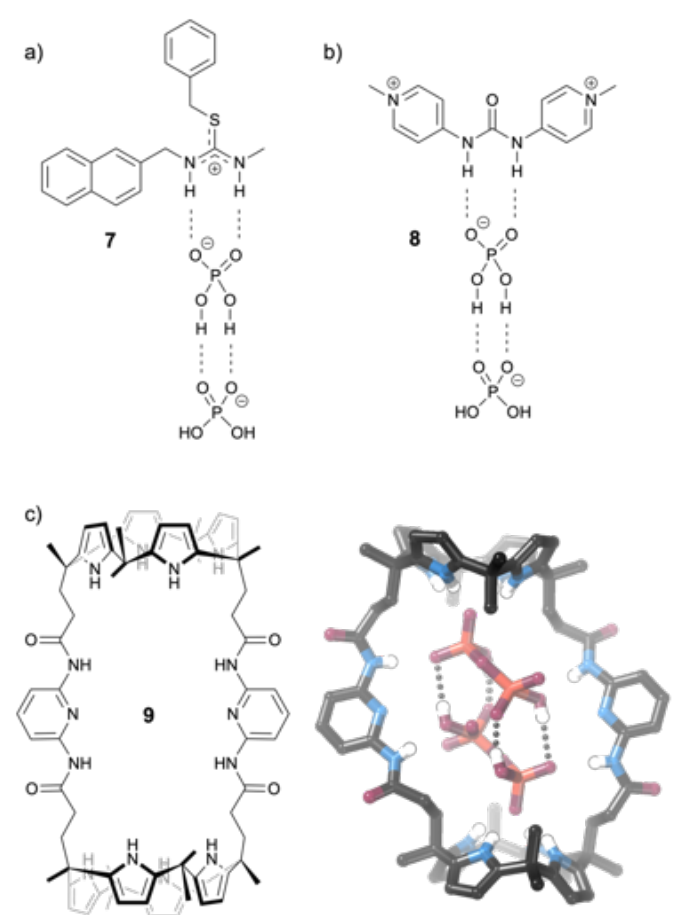


Fig. 9 a) Proposed structure of receptor **7** binding to $H_2PO_4^-$ dimer;²⁷ b) proposed structure of receptor **8** binding to $H_2PO_4^-$ dimer;²⁸ c) structure of receptor **9** and X-ray crystal structure of its complex with $(H_2P_2O_7^{2-})_2$ dimer (CSD: NEHGAL).²⁹

4.4 Isothermal Calorimetry (ITC) of Anion-Anion Dimers

ITC is used to determine the thermodynamic parameters associated with host-guest interactions including binding affinity, enthalpy change, entropy change and reaction stoichiometries, which also might provide insights into AEHBs and anion-anion dimers. In 2014, Bregović, Tomisic and coworkers³⁰ reported a study of H₂PO₄⁻ dimer recognition using a flexible thiourea based receptor **10** in acetonitrile (Fig. 10). An ITC study of the receptor **10** upon addition of H₂PO₄⁻ indicated

a 1:2 complex, which was also supported by NMR and UV-Vis titrations. The authors proposed that the 1:2 complex could be formed by either complexation of the $H_2PO_4^-$ dimer or binding of a second $H_2PO_4^-$ anion after formation of a 1:1 complex. Interestingly, ITC experiments conducted by diluting a concentrated solution of $TBA \cdot H_2PO_4$ gave a self–association constant of 2,400 M^{-1} for the dimerization of $H_2PO_4^-$ anions in acetonitrile and 50 M^{-1} in DMSO, suggesting that this association is non-negligible in even very polar solvents. Evidence of $H_2PO_4^-$ dimers in the gas phase was also obtained by electrospray ionization mass spectrometry.

Fig. 10 Structure of receptor 10 that binds to dihydrogen phosphate dimer.³⁰

In 2017, Mungulpara, Kubik and coworkers^{31,32} used ITC to study anion dimer recognition using macrocycles **11** and **12** (Fig. 11) bearing an alternating sequence of amides and triazoles. A 1:2 complex of macrocycle **11** and $H_2PO_4^-$ anion was confirmed by ITC (Fig. 11a), NMR titrations and Job plots conducted in 2.5 vol% water in DMSO. In the crystal structure, a trimer of anions was stabilized by two macrocycles forming a 2:3 complex. An expanded macrocycle **12** shows better confinement for anionanion oligomers. Either a tetramer of $H_2PO_4^-$ anions or a dimer of $H_2PO_7^{2-}$ anions was stabilized by a pair of macrocycles in the solid state (Fig. 11b). Quantitative studies using ITC and NMR suggested that the complexed phosphate dimer is also stable in competitive media (2.5 vol% $H_2O/DMSO$).

4.5 Nuclear Magnetic Resonance (NMR) Spectroscopy of Anion–Anion Dimers

Like the crystal-structure signatures for AEHBs and anion dimers, NMR spectroscopy offers the most direct evidence for receptor-assisted anion-anion dimers in solution. Key ^1H NMR resonances can be seen that originate from the O–H···O-hydrogen bonds constituting the AEHBs. In 2016, Fatila, Flood and co-workers discovered a ^1H NMR peak at 13.8 ppm in CD₂Cl₂ that was readily assigned to the hydrogen-bonded protons (O–H···O-) in the HSO₄- dimers when complexed by a pair of cyanostar macrocycles, **13** (Fig. 12). This signature was the first confirmation of receptor-stabilized anion dimers in solution. 6

The cyanostar macrocycle was created in 2013 and shows a remarkable ability to bind large anions with a characteristic 2:1 stoichiometry. Peak binding is seen for anions with a diameter of about 4.5 Å, e.g. PF_6^- , CIO_4^- . The bisulfate anion, HSO_4^- , has the right size to fit inside. When dimerized as $[HSO_4\cdots HSO_4]^{2-}$, it has a cylindrical shape with a diameter matching the cyanostar's cavity. The crystal structure confirmed 2:2 complexation between two cyanostar macrocycles and the bisulfate-bisulfate dimer. The two anions dimerize through AEHBs (Fig. 12a) with a short oxygen····oxygen distance of 2.51 Å, right at the border of Jeffrey's classification for strong hydrogen bonds set arbitrarily

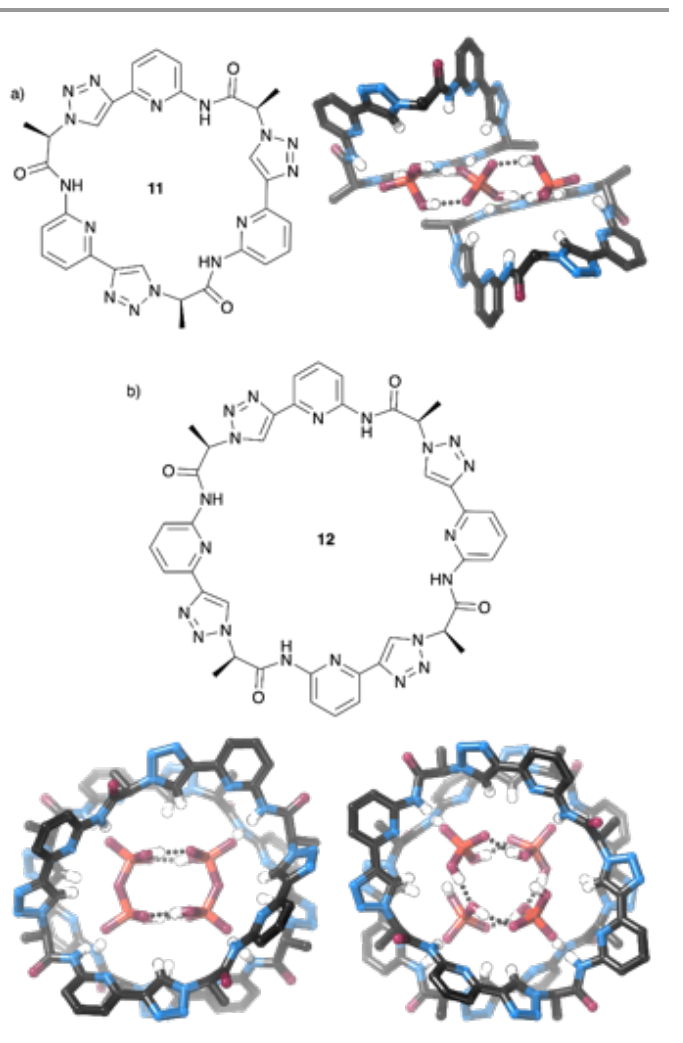


Fig. 11 a) The structure of macrocycle **11** and its crystal structure showing a trimer of dihydrogen phosphate with two macrocycles (CSD: EYUTEZ);³¹ b) The structure of macrocycle **12**, its crystal structures with dihydrogen phosphate tetramer (CSD: XAZQAT) and dihydrogen pyrophosphate dimer (CSD: XAZPOG), respectively.³²

at 2.5 Å. 33 The dimer sits inside the stacked macrocycles, which stabilize the dianion with a total of 20 CH hydrogen bonds; 10 from the cyanostilbenes and 10 from the phenylenes. NMR analysis in CD_2Cl_2 showed a characteristic peak at 12.9 ppm assigned to the OH protons of bisulfate dimers stabilized by three stacked macrocycles (Fig 12c). Upon cooling to 218 K, an extra peak at 13.7 ppm emerged and was assigned to the OH resonances of bisulfate dimers in the 2:2 complex. The ^1H - ^1H cross peaks in the NOE spectra between bisulfate and cyanostar confirmed that the bisulfate dimer is located inside the cavity of the cyanostar macrocycles in solution.

Journal Name ARTICLE

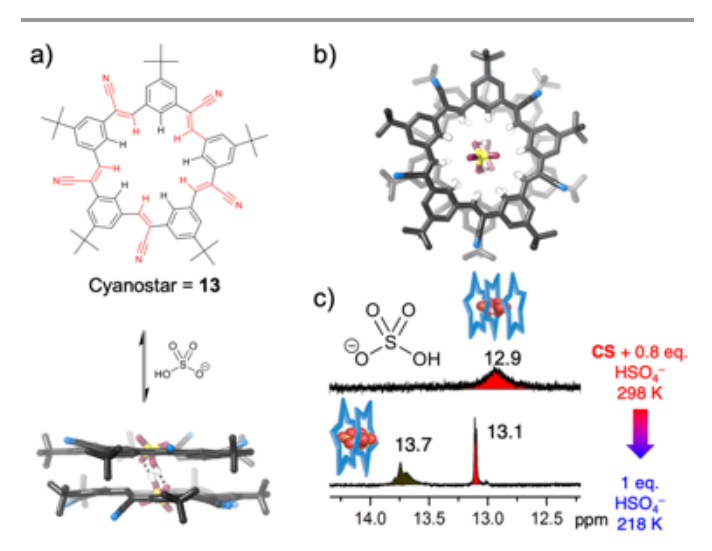
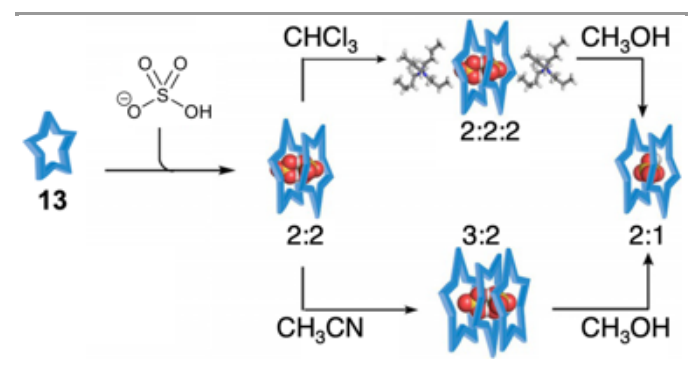


Fig. 12 a) The structure of cyanostar macrocycle **13** and the crystal structure with bisulfate-bisulfate dimer (CSD: IYEFAV), **13** $_2$ ·(HSO $_4$ -) $_2$. b) Top view of the crystal structure of macrocycle stabilized bisulfate dimer. c) Stacked ¹H NMR signatures of cyanostar encapsulated bisulfate dimers in CD $_2$ Cl $_2$ showing two and three cyanostar macrocycles stabilized bisulfate dimers. Part of figure adapted from Ref. 6 with permission from John Wiley & Sons.

Titration of bisulfate anions into a solution of cyanostar generated NMR spectra reflecting multiple complexes. ESI-MS experiments gave an initial analysis of the species distribution showing bisulfate dimers stabilized by either a double or triple stack of macrocycles. Quantitative NMR analysis showed the cyanostar-stabilized bisulfate dimer to be solvent-dependent (Fig. 13).³⁴ Specifically, a 2:2:2 complex of two macrocycles, two bisulfate anions and two tetrabutylammonium cations is observed in chloroform as a result of strong ion pairing in nonpolar solvent. Use of a more polar solvent, acetonitrile, drives conversion to the 3:2 complex on account of strong solvophobic forces originating from this macrocycle. However, with methanol added, the bisulfate dimers are not stable as either 2:2 or 3:2 complexes. Presumably, solvation does not allow formation of AEHBs with these hydroxyanions.



Phosphate displays an even richer array of assemblies (Fig. 14a) than bisulfate because the anion bears multiple hydrogen bond donors and acceptors to support oligomerization.³⁵ Complexation of dihydrogen phosphate with cyanostar always shows a mixture of species present despite attempts to tune the

driving forces using solvent, which was attributed to phosphate's pathological polymerization.

Fortunately, the distribution of cyanostar-phosphate complexes can be tuned by modifying the steric bulk of either anion or macrocycle. Zhao, Flood and colleagues found that varying phosphate substitution from a skinny butyl chain to a bulky naphthyl group enables exclusive production of the 2:2 complex in dichloromethane and in the solid state (Fig. 14b).³⁶ Surprisingly, a high-fidelity 2:2 complex is also seen when using a phosphonate hydroxyanion monosubstituted with a slim hexyl chain (C₆HPO₃⁻). Substitution of one oxygen atom in the phosphate with a methylene in the phosphonate is a small but essential steric change needed to limit the number of stacked macrocycles to just two.³⁷ Introducing bulky substituents on the cyanostar had a similar effect of limiting the stacking to favour a 2:2 complex around bisulfate dimers.³⁸

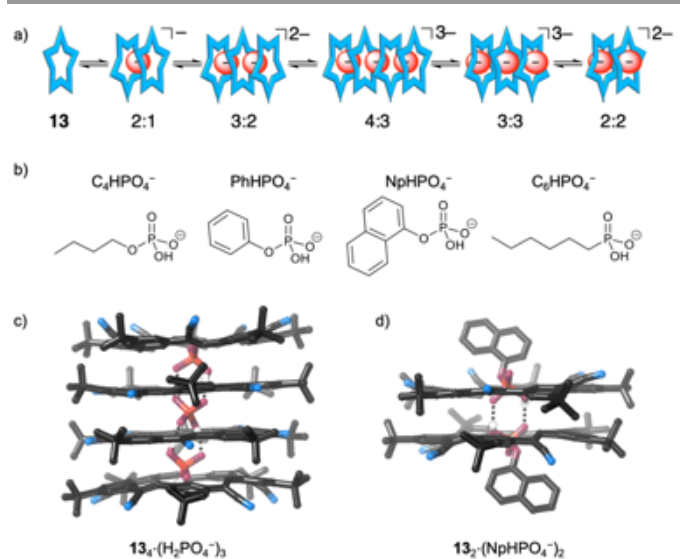


Fig. 14 a) Sequence of the main equilibria and species present in organic solution during addition of phosphate to cyanostar macrocycles; b) organophosphate and organophosphonate anions used in. self–assembly studies; c) crystal structure of cyanostar macrocycle tetramer with $\rm H_2PO_4^-$ (CSD: RERZOG); d) crystal structure of cyanostar dimer with NpHPO $\rm _4^-$ (CSD: KEIXAB). Part of figure adapted from Ref. $\rm ^{35}$ with permission from the Royal Society of Chemistry.

In 2018, Dobscha, Flood and co-workers used another size-complementary macrocycle composed of an alternating sequence of carbazole and triazole subunits called tricarb (**TC 14**) to stabilize bisulfate dimers (Fig. 15).³⁹ The crystal structure and 12–15 ppm ¹H NMR resonances verified the AEHBs. Solvent was used to switch species between a 2:2 (polar CH₃CN) and 3:2 (nonpolar solvent mixture) indicative of dipolar driving forces stemming from the stacked tricarb macrocycles.

The characteristic NMR peaks for the O–H···O⁻ hydrogen bonds verify formation of receptor-stabilized anion-anion dimers in solution from a range of hydroxyanions (Table 1) stabilized inside cyanostar and tricarb macrocycles. Splitting seen in some peaks reflects encapsulation by the well-documented diastereomers of these stacked macrocycles.⁴⁰

a) C₉H₁₉ b) C₉H₁₉ N C₉H₁₉ 14 14₂·(HSO₄-)₂

Fig. 15 a) Structure of tricarb (TC) macrocycles 14. B) Crystal structure showing the 2:2 complex between tricarb macrocycles and bisulfate dimers (CSD: HIFCEH).³⁹

The weight of examples of receptor-stabilized anion-anion dimers in solution signify the emergence of a new recognition chemistry. Clearly hydroxyanions bearing OH groups are needed but also some way to offset the Coulombic repulsions. The AEHBs have short strong hydrogen bonds. While the theoretical studies show these alone make dimers metastable, they also reveal that these self-complementary hydrogen bonds occur over short distances. Therein, we see the quandary of anion-anion attraction and repulsion is resolved when considering length scales. Ion-ion repulsion is felt over long distances, i.e., $E \propto 1 / r$, whereas the nature of hydrogen bonding is short range when considering the various forces and spans $1/r^2$ to $1/r^6$. Complexation of dimers by appropriate receptors also benefits from short range hydrogen-bond contacts in the same way, whether they stem from NH or CH hydrogen bonding. From this perspective, it appears that recognition of AEHB dimers may follow very similar rules as normal anion recognition with the added complexity of interanion self-association.

5. Applications of Anion-Anion Dimerization

5.1 Supramolecular Polymers Assembled by Receptorstabilized Anion–Anion Dimerization

Shortly after the definitive identification of AEHBs in solution, Wilson reported that aqueous solutions of tertiary ammonium bicarbonate salts aggregated into constructs at moderately high concentrations.⁴¹ The existence of bicarbonate dimers as a driving force for this assembly was implicated. While the self–assembled structures were not well-defined, demonstration of these interactions in water was important.

In order to construct well-defined supramolecular polymers, the preferred driving forces rely on well-developed and reliable recognition chemistries, e.g., hydrogen bonding, host-guest interaction and metal cation coordination. Use of anion recognition chemistry to drive supramolecular polymerization, however, is far from developed. Weak affinities and low host-guest stoichiometries are believed to limit application of anion recognition in supramolecular polymerization. Recently, two studies from Flood expanded the boundary of this field by introducing strong cyanostar-stabilized anion-anion linkages with high 2:2 host-guest stoichiometries to drive the supramolecular polymerization.^{37,42}

Inspired by the design rules used in metallosupramolecular polymers, Zhao, Flood and colleagues developed a linear supramolecular polymer based on the combination of cyanostar macrocycles and a diphosphonate monomer (Fig. 16a).³⁷ A 2:1 mixture enables facile supramolecular polymerization in dichloromethane derived from phosphonate-phosphonate dimerization (Fig. 16b). The linear polymer was confirmed from its crystal structure (Fig. 16c). In solution, the key ~14 ppm peaks (Table 1) of AEHBs were observed. Variable concentration NMR, diffusion NMR, dynamic light scattering, and viscosity studies all indicate concentration-driven supramolecular polymerization.

Table 1 Stacked ¹H NMR spectra for the signature (OH···O⁻) of the anion-anion dimer encapsulated inside stacks of macrocyclic receptors as 2:2 and 3:2 complexes.

Anion dimers	R group	Macrocycle	Position (ppm)	Condition (solvent, temp.) ^a	O–H···O⁻ NMR signature
0.00	-	13 (CS) ⁶	13.8, 13.1	CD ₂ Cl ₂ / 218 K	L
H-0	-	14 (TC) ³⁹	13.3	2:8 v/v CD ₃ CN:CDCl ₃	
*	-	14 (TC) ³⁹	13.4	CDCI ₃	ال
	⊢н	13 (CS) ³⁵	12.9	CDCI ₃	in the
	├ ~~	13 (CS) ³⁶	14.3, 14.2, 13.1	CD ₂ Cl ₂	لسلا .
O OR	$\vdash \!\!\! \bigcirc$	13 (CS) ³⁶	15.4, 15.3	CD ₂ Cl ₂	_//_
О О	$\vdash \!\!\! \subset$	13 (CS) ³⁶	15.4	CD ₂ CI ₂	_الـ
RO G		14 (TC) ³⁹	15.3, 15.2	CD ₂ CI ₂	٠
	. 🦱 👢	15 (OTgCS) ⁴²	13.8	CD ₂ Cl ₂	سالس
	H_>- 50°	15 (OTgCS) ⁴²	14.7	CD ₂ Cl ₂	lu
O R	$\vdash \sim \sim$	13 (CS) ³⁷	14.3, 14.1	CD ₂ CI ₂	
R	H+1	13 (CS) ³⁷	14.1, 13.9	CD ₂ Cl ₂	16.0 15.0 14.0 13.0 pp

a NMR spectra recorded at 298 K unless noted. * indicates the NMR signature for the anion-anion dimers encapsulated by three stacked macrocycles, 3:2 complex.

Chemical Society Reviews TUTORIAL REVIEW

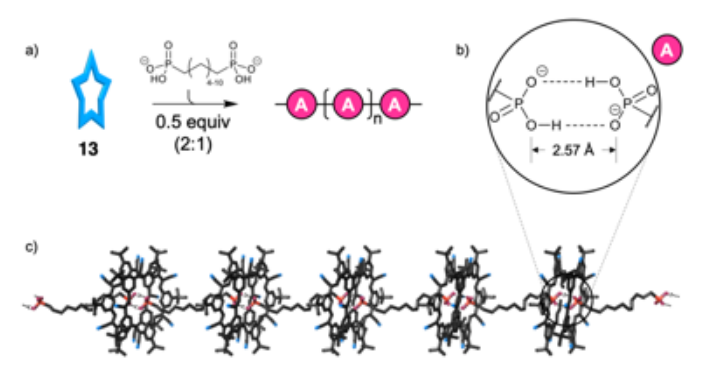


Fig. 16 a) Linear supramolecular homopolymers emerging from a 2:1 mixture of cyanostar macrocycles and alkyl diphosphonate dianions; b) the structure of the cyanostar-stabilized phosphonate dimer; c) crystal structure of supramolecular homopolymer using cyanostar and dodecylene diphosphonate (CSD: VIZFEE).³⁷

A rare correlation was seen between slow-exchange NMR data and the onset of a viscous solution at the critical polymerization concentration. The polymerization is switchable using acid and base indicating the capacity for supramolecular functionality. The simplicity of this new class of supramolecular polymer emphasizes the utility of AEHBs and anion-anion dimerization in materials chemistry.

To enable studies of the macromolecular materials properties, the solubility of the macrocycle was enhanced using triethylene glycols substituents (OTgCS, 15). When combined with a phenylene diphosphate monomer, Zhao, Flood and colleagues discovered a rare form of supramolecular polymerization controlled by reaction stoichiometry (Fig. 17a). At a 2:1 macrocycle to monomer ratio, the expected supramolecular homopolymer driven by cyanostar-stabilized phosphate dimerization (Fig. 17b) was produced. At a 1:1 ratio an unexpected alternating supramolecular copolymer was seen as verified by crystallography with two types of supramolecular linkages (labelled A and B in Fig. 17d). In one of the AEHBs, the uncomplexed dimers are stabilized by four countercations.

The two supramolecular polymers display good adhesion to the glass slides. Quantitative testing suggested the homopolymer displays adhesion comparable to superglue (polycyanoacrylate) while the alternating copolymer is weaker and similar to commercial white-glue (poly(vinyl acetate)). Thus, the material property of adhesion is correlated to the sequence and structural information encoded into these supramolecular polymers. These findings reinforce the idea that AEHBs, despite being considered weak, are actually sufficiently reliable to enable glass surfaces to be glued together.

5.2 Solid State Self–Assembly and Hydrogen Bonded Frameworks

Because AEHB anion—anion interactions have generally been considered weak, it is perhaps unsurprising that they have received little attention in the context of crystal engineering and the synthesis of hydrogen-bonded architectures. There have, however, been some notable successes which suggest that there is significant scope for further developments in this area.

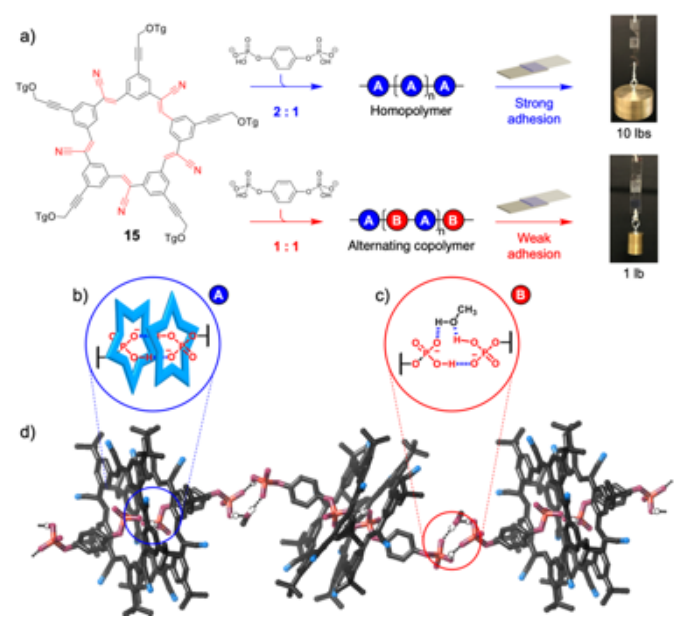


Fig. 17 a) Stoichiometry-controlled supramolecular homopolymer and alternating copolymer based on **OTgCS** macrocycles **15** and phenylene diphosphate dianions showing strong adhesion and weak adhesion, respectively. The structure of b) the cyanostar-stabilized phosphate dimer, and c) the uncomplexed phosphate dimers as the driving force for copolymerization are highlighted. d) Crystal structure of alternating supramolecular copolymer using **CS** and phenylene diphosphate (CSD: FUNLEI). Part of Figure adapted from Ref. ⁴² with permission from the American Chemical Society.

In 2000, Mak and Xue used AEHBs to prepare rosette ribbons, which consist of hexagonal rosettes that share sides to form a ribbon (Fig. 18a).⁴³ The ribbons were assembled from guanidinium cations and bicarbonate dimers, and further hydrogen bonding interactions with either terephthalate or 4-nitrobenzoate anions gave 2D anionic hydrogen bonded sheets. A follow-up paper demonstrated that the rosette ribbon motif could also be linked with other carboxylate anions, and that these structures formed in water.^{44†}

In 2010, Gong, Sessler and co-workers reported the tetracationic macrocycle **16** (Fig. 18b).⁴⁵ This macrocycle forms a pseudorotaxane with biterephthalate but not terephthalic acid or terephthalate. Solution NMR data and vapour pressure osmometry suggested that the system predominantly existed as dimer of pseudorotaxanes in solution, while crystallization led to the formation of a daisy chain pseudorotaxane.

In 2019, two reports demonstrated that it was possible to go beyond the 1D architectures reported by Gong and Sessler and form extended hydrogen bonded frameworks by combining hydrogen-bonding cations with bicarbonate dimers. In the first of these, Williams, Custelcean and co-workers showed that aqueous solutions of readily-prepared bis(iminoguanidines) absorb atmospheric CO_2 resulting in the precipitation of the bis(iminoguanidinium) as its bicarbonate salt (Fig. 19a). Crystallographic analysis revealed that these salts were highly insoluble 2D frameworks assembled by hydrogen bonding between the bis(iminoguanidinium) cations and hydrated bicarbonate dimers. Remarkably, this crystallisation process can be used to remove CO_2 from simulated flue gas. Importantly, this process is highly reversible as gentle heating of the

framework liberates CO_2 to regenerate the neutral bis(iminoguanidine) for reuse. Release of CO_2 is relatively slow at 80 °C taking two hours, but is complete within minutes above 110 °C. Kinetic measurements, optical imaging and computational studies were all consistent with a mechanism where a proton is transferred from the charged guanidiniums to the anion dimer to ultimately form a H_2CO_3 dimer, which subsequently releases water and CO_2 . Importantly, this regeneration process has a lower energy requirement than the industrial standard using monoethanolamine, and the regenerated bis(iminoguanidine) could be recycled ten times with no significant loss of activity. 46

Cullen, Gardiner and White used a tetrakis(amidinium) cation and bicarbonate anion dimers to assemble a 3D hydrogen bonded organic framework (HOF, Fig. 19b).⁴⁷ The diamondoid framework consists of a 1:1 ratio of the tetracation and dianionic bicarbonate dimer, with an additional bicarbonate dianion dimer located in the pores of the 3D HOF. Similar to Custelcean's frameworks,⁴⁶ CO₂ could be released at low temperatures, with this process occurring at temperatures as low as 75 °C in the solid state, and 50 °C with the frameworks suspended in DMSO.⁴⁷

It is noteworthy that, while many HOFs are not stable in polar organic solvents with respect to dissolution,⁴⁸ this framework is stable. Indeed, Mak's rosette ribbons,^{44††} Custelcean's 2D system,⁴⁶ and White's 3D framework⁴⁷ are all prepared in water. Use of water is remarkable given the strong hydrogen bond-disrupting ability of this solvent. Clearly, the AEHB dimers are strong enough that they can persist in the presence of water and must form to some degree in solution to allow crystallisation to occur. Notably, in all of these structures the AEHB dimer is fully saturated with hydrogen bond donors, which may account for some of this stability.

A final example of an application of AEHBs, which also functions in contact with aqueous media was reported by Valkenier, Šindelář and co-workers. They reported fluorinated bambusuril macrocycles such as **17** (Fig. 20) and showed that these were highly effective at transporting anions across lipid bilayers.⁴⁹ Notably, the hosts were highly efficient at exchanging chloride and bicarbonate ions, while unusually exchange with nitrate was significantly slower.

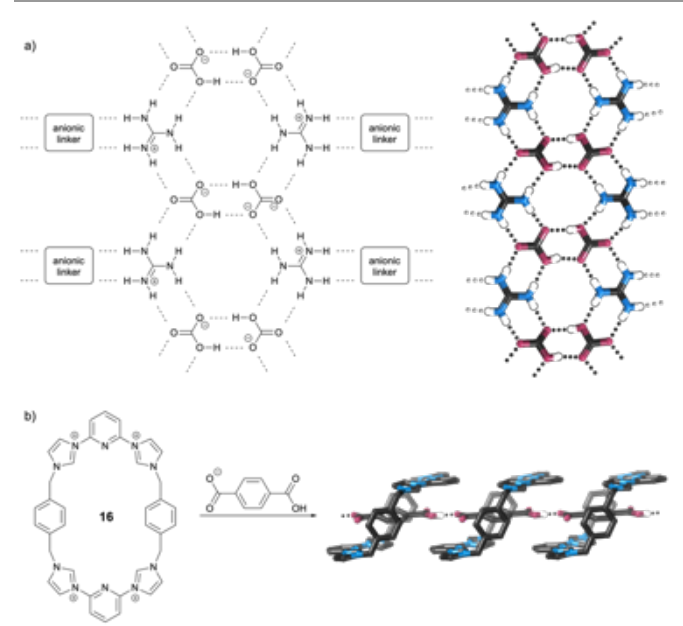


Fig. 18 (a) Structure and X-ray crystal structure of Mak's AEHB rosette ribbons, ^{43,44} which form 2D hydrogen bonded sheets by hydrogen bonding to anionic linkers (CSD: QIFFIU). (b) Structure of Sessler's tetracationic macrocycle **16** and its X-ray structure of pseudorotaxane with biterephthalate anion (CSD: VUQMOK). ⁴⁵

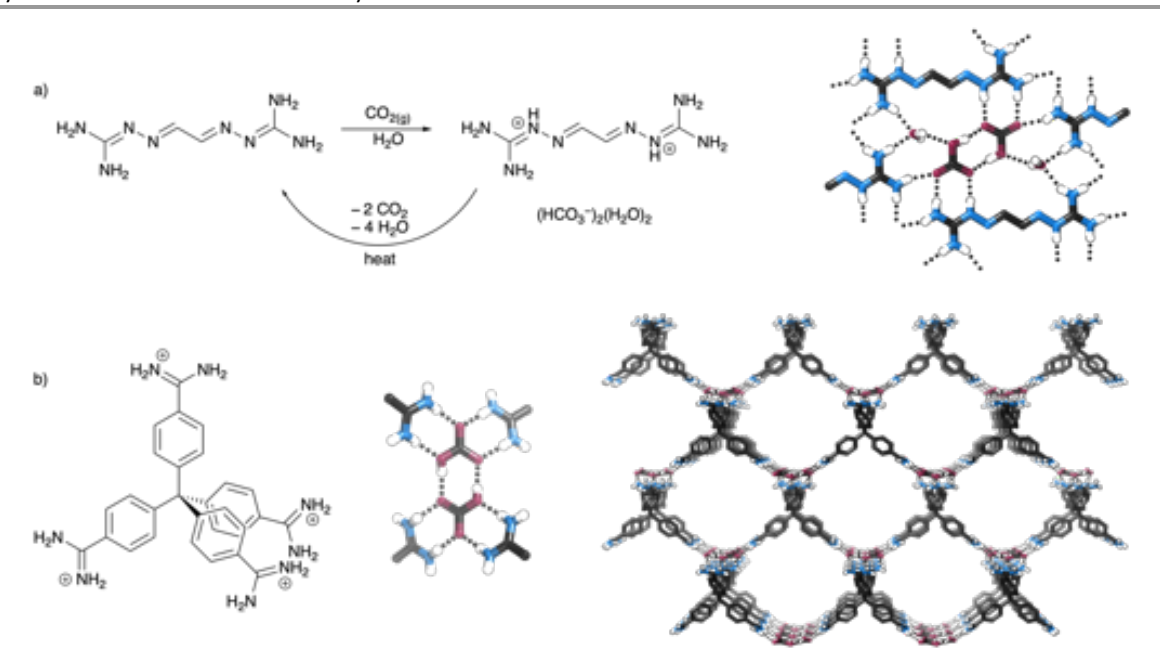


Fig. 19 Structures of extended frameworks assembled with AEHB H-bonding: a) Schematic of CO₂ sequestering process reported by Custelcean, and detail of the hydrogen bonding arrangement and the bicarbonate dimer in the crystal structure (CSD: VIWPEZ);⁴⁶ b) Structure of tetrakis(amidinium) cation used by White to prepare a 3D hydrogen bonded framework, detail of hydrogen bonding arrangements, and picture of the crystal structure (CSD: SOYRAC).⁴⁷

Chemical Society Reviews TUTORIAL REVIEW

Detailed NMR studies as well as computational studies revealed that the hosts could bind pairs of anions including bicarbonate dimers, bisulfate dimers and *hetero*-dimers of bisulfate or bicarbonate with chloride anions. The binding of this Cl⁻/HCO₃⁻ pair was used as part of the rationalization of the hosts' selective transport properties.

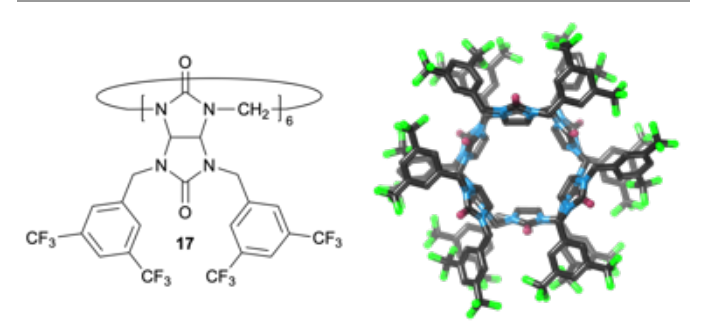


Fig. 20 Diagram and crystal structure of Valkenier and Šindelář's bambusuril macrocycle that can bind anion pairs and transport them across membranes (CSD: BIRROM).⁴⁹

6. Summary and outlook

In conclusion, anti-electrostatic hydrogen bonds (AEHBs) and the anion-anion dimers they hold together have emerged as a new recognition chemistry that is driving developments in supramolecular and materials chemistry. Contrary to expectations from Coulomb's Law, protic hydroxyanions bearing hydroxyl groups (-OH) show a surprisingly reliable facility to dimerize or oligomerize together by hydrogen bonding. AEHB anion-anion associations exist commonly in the solid state where the competition between long-range electrostatic repulsion and the short-range contacts from the hydrogen bonds in AEHB dimers is leveraged in this particular environment. Theoretical studies provide mechanistic insight into the relatively strong hydrogen bonding interactions between anions. AEHB anion-anion dimers can be stable in solution and display well-defined complexes with the help of receptor stabilization. The resulting complexes have been characterized using UV-Vis and NMR spectroscopy, and ITC. When complexation occurs by encapsulation inside either cyanostar or tricarb macrocycles, direct evidence was seen for the AEHBs by NMR spectroscopy. An OH resonance in the 12-16 ppm range signals the hydrogen-bonded anion-anion dimers. Overall, the short-range character of hydrogen bonding appears to offset the long-range repulsions from ion-ion interactions. Although these anion dimers are generally considered to be weak, they are strong enough to drive supramolecular polymerization, adhesion, and hierarchical assembly. Clearly, the investigation of AEHB anion-anion dimers is still in its infancy; to conclude we offer four points that we think are important as this area develops.

1. Fundamentals of AEHBs and anion—anion dimers
While there is much we have learned about these systems,
there is also much that we do not know. For example, the effect

of solvent on the self–association of anions is not yet well understood: while a less polar solvent will strengthen hydrogen bonding interactions, its lower dielectric constant will presumably increase the Coulombic repulsion between anions; yet this is not what appears to be seen. 18,19,30 Therefore, the relationship between solvent polarity and H-bond strength is likely to be less straightforward than is the case for a "conventional" hydrogen bond. Another pertinent question relates to the potential energy surface of anions as they approach one another. This has been well-defined in the gas phase, but is far less clear in solution and when receptors are present. Can the various interactions of anions, cations, receptors and solvent be teased apart?

2. Binding of " H_2PO_4 " by supramolecular anion receptors Solution data clearly demonstrates that H_2PO_4 anions self–associate in a range of solvents, as does bioxalate in chloroform. Presumably this is true for a range of other anions in at least some solvents (e.g. HCO_3 , HSO_4). This capacity for anion-anion dimerization needs to be taken into account when studying the binding of these anions to receptors. It is not uncommon to see complex curve shapes when H_2PO_4 is titrated with a receptor, where NMR or other signals are initially moving in one direction and then reversing. While this may be evidence for more than one host:anion binding stoichiometry, it may also be related to breaking up dihydrogen phosphate dimers and oligomers. Given the strong self–association of H_2PO_4 anions in even highly polar solvents, titration results with this anion should be interpreted with an abundance of caution.

3. Criteria for recognizing AEHBs and anion—anion dimers in solution

Pioneering computational studies have shown that anion—anion dimers (and larger aggregates) are clearly metastable in the gas phase, and their existence in the solid state is well-established. While the existence of anion-anion dimers in solution has been definitively established, this does not mean that all receptors that bind more than one H₂PO₄- (or other protic anion) necessarily bind the anion as an AEHB dimer. By definition protic anions have good H-bond donors and may well interact with receptors in other ways. We suggest that observation of an O–H···O[–] proton resonance by ¹H NMR spectroscopy is the Gold Standard in this regard, although we appreciate that this may not always be possible due to a range of factors including H/D exchange and peak broadening stemming from chemical exchange. Cooling the system or moving to a different solvent may assist in this regard. Molecular dynamics simulations, which consider both solvent molecules and cations (albeit at a low level of theory) may offer computational evidence for such interactions, and diffusion NMR studies can support the existence of anion-anion-induced aggregates. Generally, we would urge a cautious interpretation of the data available, as well as the consideration and discussion of other possible binding modes.

4. Increasing and applying complexity

While the field is still in the early stages of development, we are beginning to see applications of AEHB anion–anion dimerization, for example in supramolecular polymerization, anion transport and CO₂ capture. These findings all suggest the AEHBs are a reliable new recognition motif and we believe that the time is ripe for further developments in this area. Apart from one crystal structure and one solution study, *hetero*-anion dimers and aggregates have not yet been developed and we suggest that these are worthy of further consideration. Very recently, Huber published the first example of an *anti*-electrostatically halogen bonded (AEXB) anion–anion dimer,⁵⁰ and these and other sigma-hole interactions are also likely to have an important role to play.

Conflicts of interest

There are no conflicts to declare.

Acknowledgements

WZ and AHF acknowledge support from the National Science Foundation (CHE-1709909). WZ thanks Yusheng Chen for helping organize references. NGW thanks the Australian Research Council for funding (DE170100200), and Dr Graeme Spence (Melbourne, Australia) for preparing Fig. 4.

Notes and references

- [†]The name interanionic hydrogen bonds (IAHBs) has also been used by some authors.
- ^{††}The initial report mentioned that crystals were grown by "slow evaporation of the reactants" but did not give a solvent.
- N. Busschaert, C. Caltagirone, W. Van Rossom and P. A. Gale, Chem. Rev. , 2015, 115, 8038-8155.
- 2. H. Luecke and F. A. Quiocho, *Nature*, 1990, **347**, 402-406.
- 3. J. Kraut, Acta Crystallogr., 1961, 14, 1146-1152.
- 4. R. A. Hearn and C. E. Bugg, Acta Crystallographica Section B, 1972, 28, 3662-3667.
- 5. A. Rajbanshi, S. Wan and R. Custelcean, *Cryst. Growth Des.*, 2013, **13**, 2233-2237.
- E. M. Fatila, E. B. Twum, A. Sengupta, M. Pink, J. A. Karty,
 K. Raghavachari and A. H. Flood, *Angew. Chem., Int. Ed.*,
 2016, 55, 14057-14062, and references therein.
- 7. Q. He, P. Tu and J. L. Sessler, *Chem*, 2018, **4**, 46-93.
- 8. N. G. White, *CrystEngComm*, 2019, **21**, 4855-4858, and references therein.
- 9. M. E. Light and P. A. Gale, CSD Communication, Deposition Number: 1491437, CSD Code: IQOKOQ, 2016.
- D. Braga, F. Grepioni and J. J. Novoa, *Chem. Commun.*, 1998, 1959-1960.
- 11. T. Steiner, Chem. Commun., 1999, 2299-2300.
- M. Mascal, C. E. Marjo and A. J. Blake, Chem. Commun., 2000, 1591-1592.
- 13. S. R. Kass, J. Am. Chem. Soc., 2005, **127**, 13098-13099.
- 14. I. Mata, I. Alkorta, E. Molins and E. Espinosa, *ChemPhysChem*, 2012, **13**, 1421-1424.
- F. Weinhold and R. A. Klein, Angew. Chem., Int. Ed., 2014, 53, 11214-11217.
- I. Alkorta, I. Mata, E. Molins and E. Espinosa, Chem. Eur. J., 2016, 22, 9226-9234.

- 17. I. Mata, I. Alkorta, E. Molins and E. Espinosa, *Chem. Phys. Lett.*, 2013, **555**, 106-109.
- 18. C. W. Childs, J. Phys. Chem., 1969, 73, 2956-2960.
- 19. R. H. Wood and R. F. Platford, *J. Solution Chem.*, 1975, **4**, 977-982, and references therein.
- M. K. Cerreta and K. A. Berglund, J. Cryst. Growth, 1987, 84, 577-588.
- 21. L. S. Flatt, V. Lynch and E. V. Anslyn, *Tetrahedron Lett.*, 1992, **33**, 2785-2788.
- S. Valiyaveettil, J. F. J. Engbersen, W. Verboom and D. N. Reinhoudt, Angew. Chem., Int. Ed., 1993, 32, 900-901.
- 23. T. Wang and X.-P. Yan, *Chem. Eur. J.*, 2010, **16**, 4639-4649.
- R. Chutia and G. Das, *Dalton Trans.*, 2014, 43, 15628-15637.
- B. Wu, C. Huo, S. Li, Y. Zhao and X.-J. Yang, Z. Anorg. Allg. Chem., 2015, 641, 1786-1791.
- L. González, F. Zapata, A. Caballero, P. Molina, C. Ramírez de Arellano, I. Alkorta and J. Elguero, *Chem. Eur. J.*, 2016, 22, 7533-7544.
- 27. Y. Kubo, S. Ishihara, M. Tsukahara and S. Tokita, *J. Chem. Soc.*, *Perkin Trans.* 2, 2002, 1455-1460.
- G. Baggi, M. Boiocchi, L. Fabbrizzi and L. Mosca, *Chem. Eur. J.*, 2011, 17, 9423-9439.
- Q. He, M. Kelliher, S. Bähring, V. M. Lynch and J. L. Sessler,
 J. Am. Chem. Soc., 2017, 139, 7140-7143.
- N. Bregović, N. Cindro, L. Frkanec, K. Užarević and V. Tomišić, Chem. Eur. J., 2014, 20, 15863-15871.
- D. Mungalpara, H. Kelm, A. Valkonen, K. Rissanen, S. Keller and S. Kubik, Org. Biomol. Chem., 2017, 15, 102-113.
- D. Mungalpara, A. Valkonen, K. Rissanen and S. Kubik, Chem. Sci., 2017, 8, 6005-6013.
- 33. G. A. Jeffrey, *An introduction to hydrogen bonding,* Oxford University Press, New York, 1997.
- 34. E. M. Fatila, E. B. Twum, J. A. Karty and A. H. Flood, *Chem. Eur. J.*, 2017, **23**, 10652-10662.
- 35. E. M. Fatila, M. Pink, E. B. Twum, J. A. Karty and A. H. Flood, *Chem. Sci.*, 2018, **9**, 2863-2872.
- 36. W. Zhao, B. Qiao, C.-H. Chen and A. H. Flood, *Angew. Chem.*, *Int. Ed.*, 2017, **56**, 13083-13087.
- W. Zhao, B. Qiao, J. Tropp, M. Pink, J. D. Azoulay and A. H. Flood, J. Am. Chem. Soc., 2019, 141, 4980-4989.
- E. G. Sheetz, B. Qiao, M. Pink and A. H. Flood, *J. Am. Chem. Soc.*, 2018, **140**, 7773-7777.
- J. R. Dobscha, S. Debnath, R. E. Fadler, E. M. Fatila, M. Pink, K. Raghavachari and A. H. Flood, *Chem. Eur. J.*, 2018, 24, 9841-9852.
- 40. Y. Liu, A. Singharoy, C. G. Mayne, A. Sengupta, K. Raghavachari, K. Schulten and A. H. Flood, *J. Am. Chem. Soc.*, 2016, **138**, 4843-4851.
- J. S. McNally, X. P. Wang, C. Hoffmann and A. D. Wilson, Chem. Commun., 2017, 53, 10934-10937.
- 42. W. Zhao, J. Tropp, B. Qiao, M. Pink, J. D. Azoulay and A. H. Flood, *J. Am. Chem. Soc.*, 2020, **142**, 2579-2591.
- 43. T. C. W. Mak and F. Xue, *J. Am. Chem. Soc.*, 2000, **122**, 9860-9861.
- 44. J. Han, C.-W. Yau, C. W. Chan and T. C. W. Mak, *Cryst. Growth Des.*, 2012, **12**, 4457-4465.
- H.-Y. Gong, B. M. Rambo, E. Karnas, V. M. Lynch and J. L. Sessler, *Nat. Chem.*, 2010, 2, 406-409.
- N. J. Williams, C. A. Seipp, F. M. Brethomé, Y.-Z. Ma, A. S. Ivanov, V. S. Bryantsev, M. K. Kidder, H. J. Martin, E. Holguin, K. A. Garrabrant and R. Custelcean, *Chem*, 2019, 5, 719-730.
- 47. D. A. Cullen, M. G. Gardiner and N. G. White, *Chem. Commun.*, 2019, **55**, 12020-12023.
 - R.-B. Lin, Y. He, P. Li, H. Wang, W. Zhou and B. Chen, *Chem. Soc. Rev.*, 2019, **48**, 1362-1389.

48

Journal Name ARTICLE

- H. Valkenier, O. Akrawi, P. Jurček, K. Sleziaková, T. Lízal, K. Bartik and V. Šindelář, *Chem*, 2019, **5**, 429-444. J. Holthoff, E. Engelage, R. Weiss and S. M. Huber, *Angew. Chem., Int. Ed.*, 2020, DOI: 10.1002/anie202003083. 49.
- 50.